

Effect Bath Temperature of CdSe Thin Films Growing by Electrochemical Deposition

P. Prabukanthan^{1,*}, M. S. Sivakami²

¹Materials Chemistry Lab, Department of Chemistry, Muthurangam Government Arts College, Vellore 632002, India
pprabukanthan76[at]hotmail.com

²Department of Chemistry, K. M. G. College of Arts & Science, Gudiyattam – 635 803, India
sivakami.selvakumar2009[at]gmail.com

Abstract: *Thin film CdSe compound semiconductors have been deposited by electrochemical deposition on indium doped tin oxide (ITO) coated glass substrates under controlled temperature ranging from room temperature to 70 °C. For the as-deposited thin films, the GAXRD analysis revealed a uniform cubic phase of CdSe thin films with preferred orientation along the (200) plane and the calculated crystallite size was found to be 80 to 175nm using by Scherer method. The SEM micrographs showed that the film surface was composed of spherically shaped grains. Optical studies revealed that the as-deposited CdSe thin films have direct band transition whose value decreased from 1.68 to 1.77 eV bath temperature decreases. All different bath temperature obtained CdSe thin films have shown n-type conductivity. The effects of bath temperature on structural, morphological, optical and electrical properties of CdSe thin films were studied.*

Keywords: ECD, semiconductor, optical and electrical properties

1. Introduction

The binary II-VI (CdSe, CdS, CdTe, ZnO, ZnSe, ZnS and ZnTe) semiconductor's groups were of requisite candidates in various research areas, such as photovoltaic, energy storage and generation and so on. Additionally, these classes of materials also offer remarkable property in photocatalytic of water splitting and pollutant management. Among all, cadmium selenide (CdSe) NPs are known for they ingenious properties of photocatalytic and photo-luminescence, which adopt three different structures such as wurtzite (hexagonal), sphalerite, (cubic), rock salt (cubic) in nature. Further, CdSe NPs have a direct bandgap with 1.74 eV at ambient temperature and possesses n-type semiconductor nature, solar cells and degradation using photoreactor [1-8].

Recently, electrochemical deposition (ECD) has emerged as an economical technique for growing semiconductor films for the fabrication of optoelectronic devices. Particularly large area films of compound semiconductors for use in solar cells and display devices have been grown by ECD. The attractive features of this technique are its convenience in producing large area devices inexpensively and low temperature growth which yields sharper junctions. As ECD is an isothermal process controlled by electrical parameters, which are readily adjusted, there is good control over film thickness, morphology and composition [9-20].

In this work, we demonstrate the growth CdSe thin films on ITO coated glass substrate by ECD technique with different bath temperature. The bath temperature conditions and their effects on the morphology, optical and electrical properties of as-deposited CdSe thin films were investigated.

2. Experimental

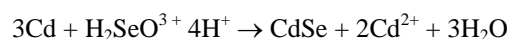
Linear sweep voltammetry (LSV) experiments were conducted in potentiostat/galvanostat CH Instruments USA,

model 604E. Electrochemical deposition (ECD) was performed in a conventional three electrode cell with ITO coated glass substrate as working electrode. The counter electrode was a Pt wire and saturated calomel electrode ($\text{Ag}^+/\text{AgCl}/\text{KCl}$) was the reference electrode. Prior to the ECD, the ITO coated glass substrates were sonicated in acetone followed by absolute ethanol for 30 min each and further rinsed with ultra pure water and finally dried at 80°C in air. As received analytical grade $\text{CdSO}_4 \cdot 7\text{H}_2\text{O}$ and SeO_2 reagents were used for the preparation of experimental solutions. We did several different conditions done, after that we could the following optimum experiment used. An electrolyte solution of optimal composition 0.3 mol dm^{-3} of CdSO_4 and 0.003 mol dm^{-3} of SeO_2 was prepared using triply distilled water. ECD was performed with different bath temperature room temperature, 40, 50, 60 and 70°C, respectively. The pH of the solution was maintained at 2 by using sulfuric acid. The electrolytic deposition potential and deposition time were maintained at -700 mV and 10 min, respectively. Furthermore, the as-deposited CdSe thin films present a reddish color when observed with the naked eye. After thin film formation, the CdSe thin films were rinsed with distilled water, dried and stored in desiccators for further studies.

3. Result and Discussion

3.1 Growth mechanism

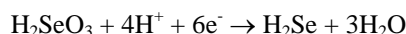
Cadmium selenide films have been formed according to the following over-all reaction 6.



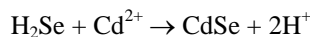
In this mechanism, the first step is the reduction of H_2SeO_3 to selenium on the surface of the substrate according to the reaction



Which is at once followed by a successive reduction process



and lastly, formation of cadmium selenide takes place according to the chemical reaction



Based electrochemistry,

$$E = E^0 + \frac{RT}{nF} \ln \frac{\alpha(\text{oxidation-state})}{\alpha(\text{deoxidize-state})}$$

where E^0 is the standard potential of the electrode system, $RT/F= 0.05917$, R the gas constant, T the experiment temperature, F the Faraday constant, n the electron amount of participation reaction, and α (oxidation- state) / α (deoxidize-state) is the ratio of the product of the all the oxidation state concentration or the disoxidation state concentration.

For iron: $n = 2$, the concentration of iron ion $\alpha (Cd^{2+}) = 0.225$ mol/L, $E^0 = -0.44$ V. At

40° C the equilibrium electrode potential can be expressed as $E(Cd^{2+}/Cd) = E^0 + (0.05917/2) \ln[\alpha (Cd^{2+})]$

$$= -0.44 + 0.02958 \ln[\alpha (Cd^{2+})].$$

While for sulfur: $n = 4$, the concentration of the thiosulphate radical ion

$$\alpha (SeO_3^{2-}) = 0.45 \text{ mol/L}, E^0 = 0.50 \text{ V}.$$

At 40° C equilibrium electrode potential can be written as

$$E(S_eO_3^{2-}/Se) = E^0 + (0.05917/4) \ln\{\alpha (SeO_3^{2-}) \times [\alpha (H^+)]^6\} = 0.50 + 0.01479 \ln\{\alpha (SeO_3^{2-}) \times [\alpha (H^+)]^6\}$$

In addition, because of the influence of the polarization action there exists some differences between the deposition potential of both iron and sulfur and the equilibrium electrode potential, which results in overpotential (the overpotential of the cathode equals to the equilibrium electrode potential minus the deposition potential). According to the experimental data, the calculated overpotential value for iron and sulfur deposited on the ITO substrates is 0.2198 and 0.8194 eV, respectively. In order to obtain FeS films, the codeposition conditions for iron and sulfur must be satisfied simultaneously. That is, their individual deposition potential is expected to be equal, where the deposition potential equals to the equilibrium potential minus the overpotential.

$$E(Cd^{2+}/Cd) - 0.2198 = E(SeO_3^{2-}/Se) - 0.8194.$$

Therefore,

$$\ln\{[\alpha (Cd^{2+})]^2 / [\alpha (SeO_3^{2-})]\} - 6 \ln[\alpha (H^+)] = 23.0156.$$

Considering the above equations, we can infer that the concentration of H^+ or the pH value of the solution has more impact on the codeposition of iron and sulfur than the concentration of Cd^{2+} and SeO_3^{2-} . Thus, when the pH value of the solution is about 1.824 and the concentration of $CdSO_4$ and SeO_2 solution is 0.225 and 0.45 mol/L, respectively ($k = 1:2$), the codeposition of iron and sulfur can be carried out to fruition.

3.2 Glancing angle X-ray diffraction (GAXRD) analysis

CdSe has two types of crystal phase, cubic zinc-blende and hexagonal wurtzite phase. Phase identification using glancing angle X-ray diffraction (GAXRD) relies mainly on the positions of the peaks in a diffraction profile and to some extent on the relative intensities of these peaks. The shapes of the peaks however contain additional and often valuable information. Figure 1 show GAXRD patterns of the as-deposited ZnSe thin films when different bath conditions at room temperature, 40, 50, 60 and 70°C, respectively.

According to the results obtained from GAXRD study, the observed peaks are due to (111), (220), (311) and (400) planes of good crystalline in nature with cubic structure. No diffraction peaks of other phases were observed of as-deposited ZnSe thin films. The GAXRD patterns of all thin films have indicated the strong reflections from the (200) plane. From the (hkl) planes, the lattice constant (a) were evaluated using the relation,

$$a = d (h^2 + k^2 + l^2)^{1/2} \quad (1)$$

where d is inter-planar spacing of the atomic plane. The calculated d -spacing values have been used to determine the lattice constant and values are also tabulated in Table 1.

Table 1: FWHM, crystallite size, micro strain, dislocation density, number of crystallites per unit are of as-deposited CdSe thin films at different bath temperatures by GAXRD

CdSe thin films deposition at different bath temperature	FWHM of XRD peak (200) (deg.)	Crystallite size (nm)	Micro-strain ($\times 10^{-3}$)	Dislocation density ($\times 10^{14}$ lines/m ²)	Number of crystallites per unit area ($\times 10^{16}$ m ⁻²)
Room temperature	0.02251	80.2	4.99	5.8	4.5
40	0.02401	84.1	5.32	6.1	4.2
50	0.02251	90.2	5.46	6.4	3.5
60	0.02598	153.1	5.76	6.5	3.2
70	0.02891	175.1	6.41	6.9	2.8

Table 1 lists the full width at half maximum (FWHM) values of (200) diffraction peak for as-deposited ZnSe thin films at different bath temperature. The FWHM of the GAXRD peak for higher temperature as-deposited ZnSe thin film samples are higher than that of as-deposited at lower temperature ZnSe thin film samples. The reason may be due to reduction in strain. The increase of the crystallite size and the improvement of the crystallinity are responsible for the decreasing the resistivity due to grain boundary scattering. The average crystallite size (D) was evaluated from the FWHM of the (111) diffraction peak using Scherrer's equation, $D = 0.9 \lambda / \beta \cos\theta$ where β is the FWHM of the

diffraction line in radians and λ is the X-ray wavelength. The calculated average crystallites sizes were found to be in the range 84-174 nm and these are listed in Table 1. The crystallite size is found increase gradually with bath temperature increase. It may attribute that crystallite size increase with increase of deposition rate, stress and degrading crystalline nature. The micro strain (ϵ), dislocation density (δ) and number of crystallites per unit area (N) were calculated using the following relation and their values are given in Table 1.

$$\text{Micro strain } (\epsilon) = \beta \cos\theta/4 \quad (2)$$

$$\text{Dislocation density } (\delta) = 15\epsilon/aD \quad (3)$$

$$\text{Number of crystallites } (N) = t/D^3 \quad (4)$$

where θ is Bragg's angle and t is thickness of the film. In general, the crystallite size is indirectly proportional to micro strain. The decrease of ϵ and δ at both temperature lower may be due to movement of interstitial Cd atoms from inside the crystallites to its grain boundary which dissipate leading to reduction in the concentration of lattice imperfections. Number of crystallites (N) is increasing with bath temperature, which may be attributed to the reduction in crystallite size.

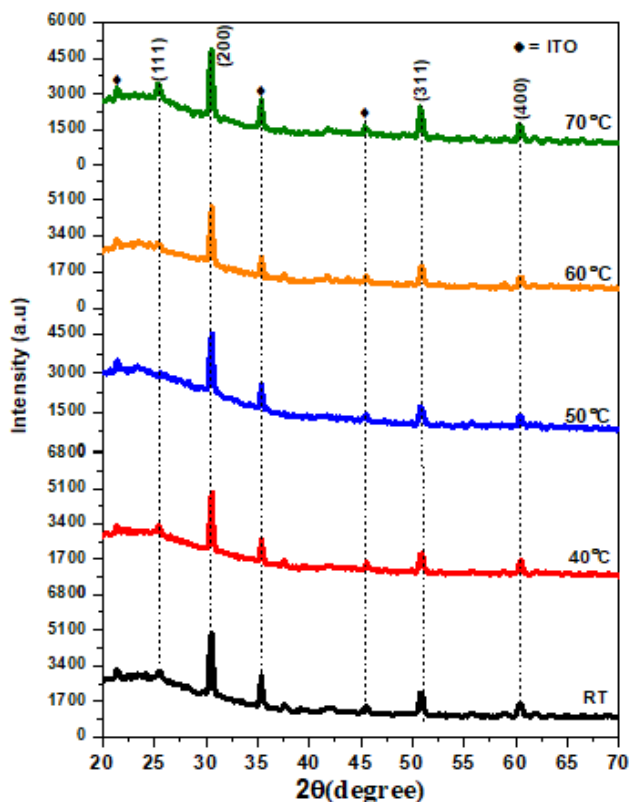


Figure 1: GAXRD patterns of CdSe thin films deposited different bath temperatures

3.3 UV-Visible Spectral Studies

Absorption coefficient (α) were estimated from a absorption spectra in as-deposited CdSe thin films at different bath temperature. Figure 2 shows the $(\alpha hv)^2$ vs photon energy. For

the as-deposited CdSe thin films at lower bath temperature sharp absorption coefficient edge was observed at 1.68 eV to 1.77 eV. The band gap is changed for as-deposited ZnSe thin films at higher bath temperature. It may be observed that fall of absorption coefficients with the wavelength of incident radiation at the absorption coefficient edge is sharper for as-deposited CdSe thin films at bath temperature lower.

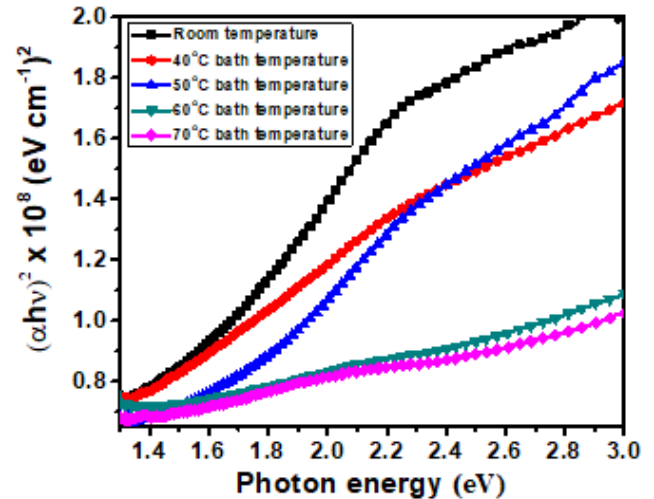


Figure 2: $(\alpha hv)^2$ vs hv plots of CdSe thin films at different bath temperatures

3.4 Photoluminescence (PL) Studies

The room temperature photoluminescence (PL) spectra of as-deposited CdSe thin films are shown in Figure 3. PL spectra of as-deposited CdSe thin films taken by us excitation wavelength (λ_e) have 325 nm. It shows broad band emission which is due to deep level emission. The as-deposited ZnSe thin films at different bath temperatures were band to band transition peak at 419 nm (2.96 eV).

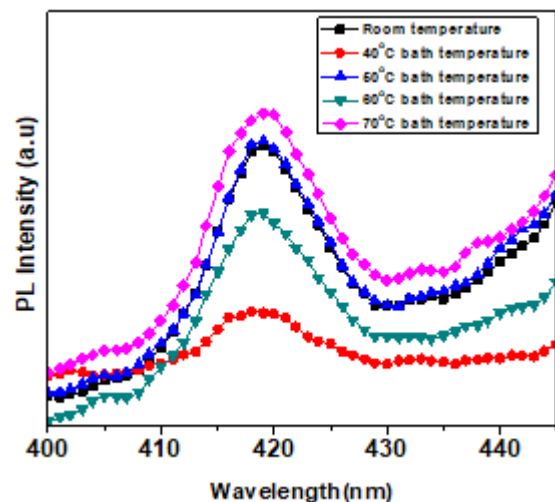


Figure 3: Photoluminescence spectra of CdSe thin films at different bath temperatures

3.5 Morphology studies

Scanning electron microscopy (SEM) is an excellent method to study the morphology of the samples. Figure 4 (a-e) show SEM images of the as-deposited and annealed CdSe thin

films. The films were uniform and cover the ITO substrate surface nicely. It is interesting to note that the as-deposited CdSe thin films seem to be composed of densely packed spherical nanoclusters 300 - 700 nm in size consisting of a

number of spherical nanosized grains. This clearly suggests that the growth of the CdSe films takes place via cluster by cluster deposition, (i.e.) aggregation of colloidal particles formed in the solution rather than via ion by ion deposition.

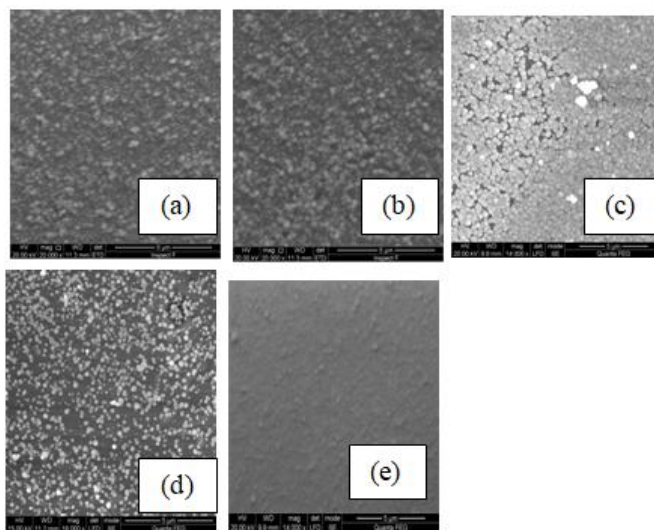


Figure 4 (a-e): SEM images of as-deposited CdSe thin films at different bath temperature (a) room temperature (b) 40°C (c) 50°C (d) 60°C (e) 70°C

3.6 Electrical studies

Conductivity type, resistivity, carrier concentrations, electron mobility measurements were made for the as-deposited CdSe thin films at different bath temperature by Hall effect apparatus with van der Pauw configuration. All the as-deposited CdSe thin films are seen to have n-type conductivity. Resistivity, carrier concentration, electron mobility values of the films are given in the Table 2. The electrical resistivity of as-deposited CdSe thin film was of the order of $10^4 \Omega\text{cm}$ which was decreased to $10^3 \Omega\text{cm}$ bath

temperature increased. The higher value of resistivity may be attributed to nanocrystalline or amorphous nature of thin film or grain boundary discontinuities, presence of surface states and less roughness of CdSe films. The electron mobility and carrier concentrations were higher for high bath temperature. The higher value of electron mobility and carrier concentrations of higher bath temperature CdSe thin films which leads to a partial screening of the polar vibrations stimulated by mixed phase, improvement in crystallite size and decrease in density of grain boundary intercrystallite of the charge carriers.

Table 2: Conductivity type, resistivity, carrier concentrations, electron mobility measurements were made for the as-deposited CdSe thin films at different bath temperature (room temperature 70°C) by Hall Effect apparatus

Sl. NO.	CdSe thin films deposited at bath temperature	Type of conductivity	Resistivity (cm)	Carrier Concentrations ($\times 10^{21} \text{cm}^{-3}$)	Electron mobility ($\text{cm}^2\text{VS}^{-1}$)
1	Room temperature	n	3.4×10^4	20	36
2.	40°C	n	2.9×10^4	21	42
3.	50°C	n	2.8×10^4	19	41
4.	60°C	n	1.2×10^3	18	44
5.	70°C	n	1.0×10^2	17	52

4. Conclusion

Cadmium selenide (CdSe) thin films have been deposited on indium doped tin oxide coated glass substrate from an aqueous electrolytic solution by electrochemical deposition (ECD) technique. The experiment carried out different bath temperatures. The SEM results represent that the films as-deposited at lower temperature have surface with spherical-shaped grains and films were uniform with particles, appeared crystallite in nature with smooth homogeneous morphology and well covered on the substrate. EDAX analysis suggest that the as-deposited ZnSe thin film at lower temperature has a near stoichiometric. The presence of the GAXRD pattern represents that the as-deposited ZnSe thin films all were

found that good crystalline in nature. Each film shows a preferred orientation along (200) plane in addition to other two prominent planes (220) and (311), respectively. The microstructural parameters such as crystallite size, microstrain, dislocation density and number of crystallites per unit area were estimated from GAXRD data. The crystallinity and surface structure of the thin film strongly influence the optical properties. Thus the absorption coefficient and the stronger PL intensity of as-deposited ZnSe thin films at higher bath temperatures.

References

- [1] L. Shanying, Z. Haipeng, T. Damin, Mater. Sci. Semicond. Process. 16 (1) (2013) 149–153.
- [2] Y. A. Kalandaragh, A. Khodayari, Mater. Sci. Semicond. Process. 13 (4) (2010) 225–230.
- [3] A. Fujita, A. Ota, K. Nakamura, Y. Nabetani, T. Kato, T. Matsumoto, Mater. Sci. Semicond. Process. 6 (5–6) (2003) 457–460.
- [4] S. K. Haram, B. M. Quinn, A. J. Bard, J. Am. Chem. Soc. 12 (2001) 8860–8861.
- [5] Z. L. Wang, X. Y. Kong, Y. Ding, et al. , Adv. Funct. Mater. 14 (2004) 943–956.
- [6] S. Datta, B. Das, Appl. Phys. Lett. 56 (1990) 661–665.
- [7] L. Zhao, L. Hu, X. Fang, Adv. Funct. Mater. 22 (2012) 1551–1566.
- [8] H. Choi, J. G. Radich, P. V. Kamat, J. Phys. Chem. Lett. 118 (2013) 206–213
- [9] T. Rajesh Kumar, P. Prabukanthan, G. Harichandran, R. A. Senthil, T. Arunkumar and J. Theerthagiri, Ionics, (2019) In press.
- [10] P. Prabukanthan, S. Thamaraiselvi and G. Harichandran, J. Theerthagiri, J. Mat. Sci. Mat. Electro. 30 (2019) 3268-3276
- [11] T. Rajesh Kumar, P. Prabukanthan, G. Harichandran, J. Theerthagiri, J. Mat. Sci. Mat. Electro. 29 (2018) 5638-5648
- [12] P. Prabukanthan, R. Lakshmi, G. Harichandran, T. Tatarchuk, New J. Chem. , Vol. 42 (2018) 11642-11652.
- [13] P. Prabukanthan, S. Thamaraiselvi and G. Harichandran, J. Mat. Sci. Mat. Electro. , 29 (2018) 11951-11963
- [14] T. Rajesh Kumar, P. Prabukanthan, G. Harichandran, J. Theerthagiri, T. Tatarchuk, J. Solid State Electrochem. , 22 (2018) 1197-1207
- [15] P. Prabukanthan, R. Lakshmi, T. Rajesh Kumar, S. Thamaraiselvi, Adv. Mat. Proc. , 2 (2017) 521-525.
- [16] P. Prabukanthan, T. Rajesh Kumar and G. Harichandran J. Mat. Sci. Mat. Electro. , 28 (2017) 14728-14737
- [17] T. Rajesh Kumar, P. Prabukanthan, G. Harichandran, J. Theerthagiri Ionics, Vol. 23 (2017) 2497-2507.
- [18] P. Prabukanthan, S. Thamaraiselvi and G. Harichandran, J. Electrochem. Soc. , 164 (2017) D581-D589.
- [19] P. Prabukanthan, T. Rajesh Kumar and G. Harichandran, Mat. Res. Exp. , 2 (2015) 096102
- [20] P. Prabukanthan and G. Harichandran J. Electrochem. Soc. , Vol. 161 (14) (2014) D736-D741